Dielectric Relaxation Spectroscopy of Modern Hybrid Insulation Systems

Peter Havran[1], Roman Cimbala[1], Samuel Bucko[1], Juraj Kurimský[1], Bystrík Dolník[1], Michal Rajňák[1,2], Jozef Király[1], Katarína Paulovičová[2]

[1]Faculty of Electrical Engineering and Informatics, Technical University of Košice, Letná 9, 04200 Košice, Slovakia; peter.havran@tuke.sk; roman.cimbala@tuke.sk; samuel.bucko@tuke.sk; juraj.kurimsky@tuke.sk; bystrik.dolnik@tuke.sk; michal.rajnak@tuke.sk; jozef.kiraly@tuke.sk

[2]Institute of Experimental Physics SAS, Watsonová 47, 04001 Košice, Slovakia; rajnak@saske.sk; paulovic@saske.sk

Abstract: The constant optimization of the properties of insulating materials, is currently highly topical, at a global scale, as it directly concerns the efficiency of the operation of electrical equipment. This study includes research on modern insulation systems based on hybrid and non-hybrid nanofluid-paper. Cellulose insulation is impregnated with Shell Diala S4 ZX-1 transformer oil, enriched with two types of Fe3O4 and C60 nanoparticles, with varying nanoparticle concentrations. Samples of insulating materials are subjected to analysis using the method of dielectric relaxation spectroscopy in the frequency domain. The results point to electrophysical processes, of a conductive and polarizing nature. The increasing concentration of Fullerene nanoparticles, causes a decrease in dielectric losses and reduces the influence of interfacial polarization and electric double layer polarization in the hybrid nanofluid-paper system. The loss spectra of the complex electric modulus are the same as the spectra of the complex permittivity in the liquid-paper system. The Havriliak-Negami function reveals the dominance of polarization losses over conduction losses in the studied frequency spectrum and their origin when an external alternating electric field is applied.

Keywords: frequency domain; magnetic nanoparticle; fullerene nanoparticle; fluid-paper

1 Introduction

Transformers in electricity system are one of key devices for a safe operation of the grid. There is a great danger of economic and material damages in case of their failure or damage [1] [2]. Therefore, it is necessary to keep the device in operation without overloads due to high powers, short circuits, etc. [3]. More frequent

overloads of transformers have a negative impact on their isolation system on which the lifetime of a transformer is dependent on. It is possible to detect an increasing trend in the degradation of the system in time by an appropriate monitoring of an isolation system using one of the diagnostic methods. The isolation system in transformers is composed of the combination of liquid and solid dielectric: insulating liquid and paper [4]. Another requirement for this system is also from the view of a heat convection which arises in the area of the transformer winding. Conventional insulating liquids include mineral oils, synthetic esters and natural esters. The latest requirements to increase the performance of transformers and to decrease their dimensions are a motivation for scientists and engineers to discover new approaches and methods in the field of insulating materials.

One of the ideas is to use the nm-sized particles which are freely dispersed in an insulating liquid. This method is able to increase the thermal conductivity of a particular liquid significantly and, as it is proved in certain studies, the liquid breaking strength [5]. Among the materials from the point of view of conductivity, both insulators and semi-conductive and conductive materials are used [6]. Since there is a strong magnetic field in the winding area, the usage of magnetic nanoliquids, where the paramagnetic nanoparticles are used, is considered. Given that the magnetization gradient is opposite to the magnetic field gradient, it is possible to create a natural circulation of a liquid in the transformer vessel [7].

In numerous studies, Fe_3O_4 nanoparticles prepared by a chemical method have been used to create a magnetic liquid. Subsequently, a surfactant is applied to the surface of the nanoparticles formed in this way, which prevents the nanoparticles from joining each other in the carrier liquid. The more detailed procedure for the production of nanofluid with Fe_3O_4 particles is described in [8].

Fullerene is another progressive material which has been used in experiments over last decade. This work was inspired by [9], where samples of nanofluids with Fe_3O_4 nanoparticles with added fullerene were used.

Many of the mentioned studies which deal with electrical properties observe changes in properties only at the level of a liquid material. From the point of view of applicability, it is important to carry out also experiments in the presence of paper or cellulose products, which are a part of the entire insulation system.

2 Experiment

2.1 Investigated Materials

The experiment was carried out on samples of cellulose paper that were impregnated with samples of insulating nanofluids. The carrier-impregnating

substance consisted of modern Shell Diala S4 ZX-1 transformer oil. It is a base oil that is produced by converting natural gas into liquid hydrocarbons using GTL technology (Gas to Liquid). Natural gas continues in the production process by producing synthesis gas, which is subsequently transformed into crystal clear base oil with excellent properties through Fischer-Tropsch synthesis and refining. The progressivity of this oil points to zero sulfur content, which eliminates the risk of copper corrosion in power transformers and other significant properties include, higher thermal conductivity, higher oxidation stability and lower viscosity at low temperatures. Higher oxidation stability causes more excellent resistance of the oil to aging, which is accompanied by the higher formation of acids and oxidation processes. Suppressing these adverse factors with the acceptable properties of Shell Diala S4 ZX-1 oil helps extend cellulose insulation's life in power transformers [10] [11].

Six samples with different combinations of nanoparticle concentrations were prepared. Two types of nanoparticles were dispersed into the first three samples. Magnetic Fe_3O_4 nanoparticles were precipitated from an aqueous solution of Fe_{2+} and Fe_{3+} ions with NH_4OH at 81 °C. Subsequently, steric stabilization took place using one layer of oleic acid $C_{18}H_{34}O_2$. The second type of nanoparticle consisted of a spherical molecule of carbon C_{60} (Buckminsterfullerene) with triple-bonded atoms representing a closed structure. Purchased fullerene powder with a density of 1600 kg/m^3 was homogeneously dispersed in base oil without surfactant (surface-active substance). Finally, stabilized magnetic nanoparticles with a concentration of 2.3 %w/V were added to the first three samples with a concentration of fullerene nanoparticles of 0.01 %w/V, 0.02 %w/V, and 0.03 %w/V (the ratio of the weight of the nanoparticles to the volume of the liquid). The given dispersion created a final concentration of magnetic nanoparticles of 0.01 %w/V in the investigated samples. These samples were mixed at 60 °C, and we call them hybrid nanofluids (HIN, plus HIN-P paper). Other fluid samples are non-hybrid nanofluids (NIN, plus NIN-P paper). The fourth sample is enriched exclusively with fullerene nanoparticles with a concentration of 0.01 %w/V without surfactant. The fifth sample represents pure ferrofluid with a concentration of 0.01 %w/V, which represents comparison with the other samples due to the concentration of magnetic nanoparticles. The sixth sample consists of pure Shell Diala S4 ZX-1 transformer oil with a low density of 786 kg/m^3. An overview of the investigated samples of hybrid and non-hybrid liquids, which fulfill the function of impregnation medium for cellulose insulation, is presented in Tab. 1. Impregnation of liquids and cellulose insulation took place in Petri dishes.

Table 1
Samples of impregnation nanofluids

Sample	**Concentration of fullerene nanoparticles C_{60} (%w/V)**	**Concentration of magnetic nanoparticles Fe_3O_4 (%w/V)**
	without surfactant	with surfactant – oleic acid $C_{18}H_{34}O_2$
1.	0.01	0.01
2.	0.02	0.01
3.	0.03	0.01
4.	0.01	0
5.	0	0.01
6.	0	0

2.2 Experimental Procedure

Samples of the insulation system hybrid nanofluid-paper and non-hybrid nanofluid-paper were investigated by the method of dielectric relaxation spectroscopy in the frequency domain. Dielectric relaxation spectroscopy is a non-destructive method that applies an electric field to a material to capture a small signal of the dielectric response in the form of dipole rotation and migration of free charges across the material. This modern method approximates the behavior of electrophysical parameters without the potential damage to the material caused by the application of high electric field intensities. Therefore, it is necessary to use professional measuring devices for the experimental procedure. The measurements of the samples examined by us were carried out using the IDAX 300 measuring device. This device applies an alternating electric voltage $\underline{U}$ to the material with a changing frequency $\underline{f}$ from 0.1 mHz to 10 kHz. It measures the alternating electric current $\underline{I}$ flowing through the material. From these input parameters, the measuring device calculates impedance $\underline{Z}$, from which several other electrophysical parameters are further expressed, such as, for example, electrical resistance $\underline{R}$, complex capacitance $\underline{C^*}$, dissipation factor $\underline{tan\,\delta}$, and electrical conductivity $\underline{\sigma}$. The output from the IDAX 300 meter was connected to a high-voltage and a low-voltage electrode. The electrode system consisted of Rogowski electrodes with a diameter of 54 mm, between which the tested hybrid and non-hybrid nano liquid-paper insulation system samples were inserted. The distance between the electrodes was 0.42 mm, representing the thickness of the cellulose insulation. The electrode system was placed in a shielded container, which was connected to the grounding of the measuring apparatus. Because wide-range frequencies were applied, the shielded container served as protection against electromagnetic frequencies from the outside environment. These unwanted frequencies could cause interference and deterioration of the quality of the measured data. To measure the samples, an alternating electric voltage of 100 V, was applied with the IDAX 300 measuring

device, which created an alternating electric field intensity of 238 kV/m at the given distance between the electrodes. The measuring apparatus is shown in Fig. 1.

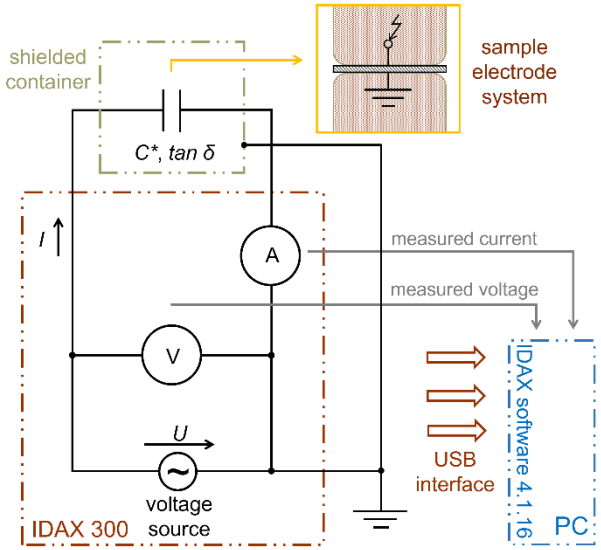

Figure 1
Experimental setup

The experimental procedure was exposed in the laboratory to an air pressure of 1013hPa, an air humidity of 36%, and an air temperature of 21 °C. The research began with the assembly of the experimental setup, which was connected according to Fig. 1, and proceeded to measure the nanofluid-paper samples. Due to the higher intensity of the electric field, the frequency band was shortened to 1 mHz – 3 kHz because it was impossible to measure the frequency spectrum of 3 kHz – 10 kHz. The reason was decreased capacitive reactance and increased electric current, which loaded the voltage source in the IDAX 300 measuring device. The measuring device recorded the measured data of the capacitance $\underline{C}$ and the dissipation factor $\underline{tan\ \delta}$ via a USB bus connected to a computer with the IDAX 4.1.16 software. Since electrophysical parameters such as capacitance $\underline{C}$ and dissipation factor $\underline{tan\ \delta}$ are mostly applied in technical practice [12], for a more accurate description of dielectric behavior within the research area, these data were converted to complex permittivity $\underline{\varepsilon^*}$, i.e., to its real $\underline{\varepsilon'}$ and imaginary component $\underline{\varepsilon''}$. The reason for using complex permittivity to describe electrophysical processes was the modeling of relaxation and conduction mechanisms according to the characteristic response function, which reflected the parameters of the distribution of relaxation times. From recent studies, it was also found that the complex electric modulus $\underline{M^*}$, as the inverse value of the complex permittivity $\underline{\varepsilon^*}$, can point out in detail the dynamics of the distribution of polarization processes by eliminating the conduction process that

is present in the low-frequency band [13]-[16]. Therefore, the complex electric modulus $\underline{M^*}$ and the complex permittivity $\underline{\varepsilon^*}$ will be used to analyze hybrid and non-hybrid nanofluid-paper samples.

3 Results and Discussion

The results of the experiment are analyzed in this section. We present the results of the complex permittivity, which will be accompanied by the results of the complex electric modulus for a comprehensive description of the investigated materials. In the third part of this chapter, electrophysical processes will be captured and analyzed through the distribution of relaxation times according to the Havriliak-Negami dielectric model.

3.1 Complex Permittivity

The complex permittivity of samples of hybrid and non-hybrid nanofluids forming an insulating system together with cellulose paper is presented in this section. In Fig. 2, we present the real permittivity in the frequency band 1 mHz – 3 kHz. In the case of samples containing magnetic nanoparticles, a low-frequency dispersion is captured, which is attributed to at least one relaxation phenomenon. In higher frequencies, the real permittivity is stable at the value of 2.2 with a slight decrease. The exception is the 5. and 3. samples with a 1.07 times higher value, i.e., the sample with zero and the highest concentration of fullerene nanoparticles (0.03 %w/V). 6. the paper sample impregnated with pure GTL oil has the lowest real permittivity, moving at the value level of 2.2. The effect of fullerene nanoparticles is manifested by an increase in the real permittivity by a value of 0.04 in the entire frequency spectrum.

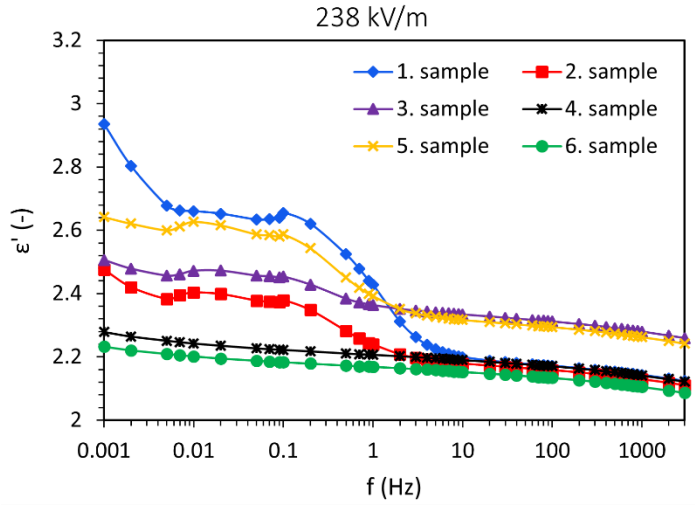

Figure 2
The frequency-dependent real permittivity $\varepsilon' = f(f)$ of the investigated samples

In Fig. 3, we present the imaginary permittivity in the examined frequency band. As mentioned in the characteristics of real permittivity, samples containing magnetic nanoparticles show a clear dielectric relaxation in the low-frequency and medium-frequency bands, which confirms the imaginary permittivity spectrum. Samples 1, 2, 3, and 5, i.e., samples with magnetic nanoparticles, reflect a remarkable loss maximum in the band 0.1 Hz – 1 Hz, which subsequently changes to increasing dielectric losses again as the frequency decreases. Comparing the HIN-P samples, an inverse decrease of the relaxation maximum with increasing concentration of fullerenes can be seen. In addition to the reduction of the relaxation peak, the captured mechanism is shifted to lower frequencies. This exciting feature reduces dielectric losses at 50 Hz and 60 Hz operating frequencies, representing important information in applying the given insulation system. The samples without magnetic nanoparticles (4 and 6) do not show a relaxation maximum at a frequency of 1 Hz. However, their dielectric losses increase in the low-frequency band, similar to the other samples. The mentioned increase in dielectric losses can be caused by conduction losses manifested in the low-frequency band. The fullerene fraction in the GTL carrier oil in the fluid-paper system (4 sample) slightly increases the dielectric loss and the real permittivity compared to the oil-paper sample (6. sample).

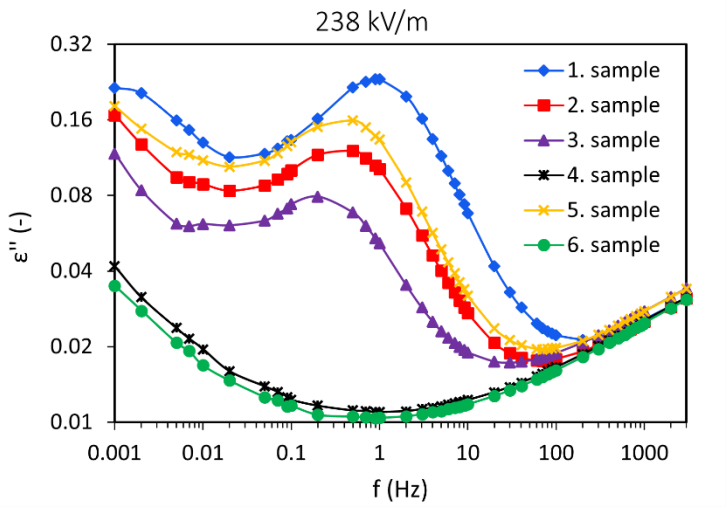

Figure 3
The frequency-dependent imaginary permittivity $\varepsilon'' = f(f)$ of the investigated samples

The complex permittivity diagram in the complex plane is shown in Fig. 4. In the given display, the measured values of ε'' are plotted as a function of ε' at different frequencies (1 mHz – 3 kHz). If the individual measured points in this diagram belong to a semicircle, then the given insulating system reacts to the external electric field with a relaxation response. In practice, very few materials exhibit a single polarization mechanism with a relaxation time, so that this fact can be attributed to the distribution of relaxation times. From plotting the complex permittivity to the complex plane, we can observe for samples with magnetic nanoparticles an indication of the development of the curves into a semicircle, which corresponds to the relaxation peaks of the imaginary permittivity. Samples without the magnetic nanoparticle fraction have V-shaped characteristics, while it is not known whether the low-frequency increase is caused by a relaxation or conduction process. We also encounter a similar dilemma with samples 2, 3, and 5. The HIN-P sample with the same concentration of fullerenes and magnetic nanoparticles 0.01 %w/V (1 sample) copies a certain imaginary semicircle in the low-frequency band, which would reflect the presence of a relaxation phenomenon. Based on the development of the measured permittivity spectra into a complex plane, it is not possible in our case to accurately characterize electrophysical processes at the molecular level. Because of this, the complex permittivity values were recalculated to the values of the complex electric modulus, as an inverse complex dielectric parameter.

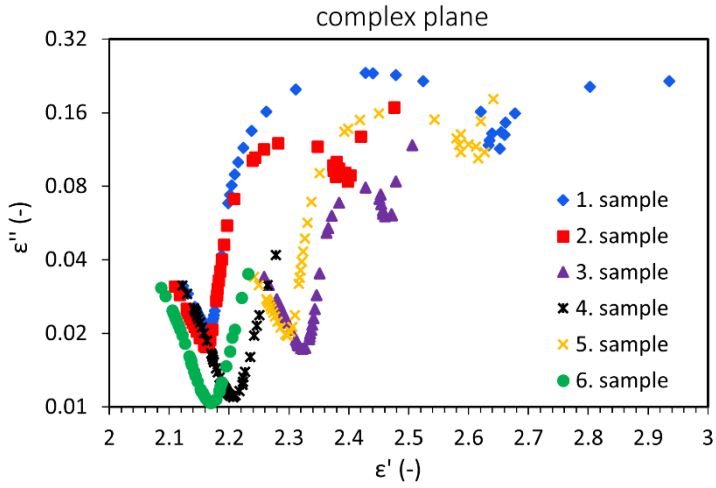

Figure 4
Complex permittivity in the complex plane *ε´´=f(ε´)*

3.2 Complex Electric Modulus

The complex electric modulus is widely known due to its property of presenting the studied material without the influence of the conduction process and electrode polarization. These processes can affect the low-frequency spectrum of dielectric losses, which would distort the analysis of the measured data, presenting inaccurate identification of electrophysical processes in the low-frequency range. Some electrotechnical equipment, working on the principle of direct current, shows a failure rate based on the failure of the insulation system. Therefore, it is necessary to accurately identify electrophysical processes in the low-frequency band with subsequent prediction or provide relevant information to improve the insulation system. Fig. 5 shows the frequency spectra of the real modulus. Compared with the real permittivity in Fig. 2, the exact shape of the characteristics can be seen, which are reversed. It is possible to proceed from the findings that were described in subsection 3.1.

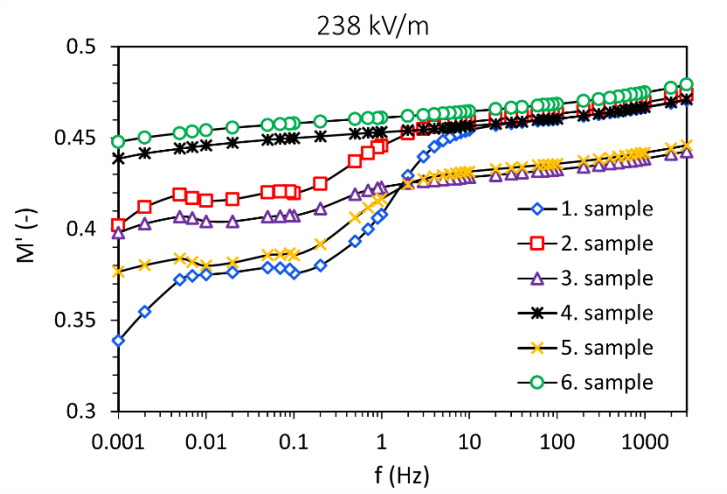

Figure 5
The frequency-dependent real modulus $M'=f(f)$ of the investigated samples

The complex electric modulus shows the dielectric behavior of the investigated materials exclusively from the point of view of relaxation processes. This means that it only provides the relaxation response of the investigated material, excluding the electrode polarization. Fig. 6 represents an insight into the loss spectra of a complex electric modulus. When comparing the frequency dependences of ε'' and M'' of liquid insulation (oils, nanofluids), M'' has a shifted relaxation mechanism to the band of higher frequencies [8] [13]. From Fig. 3 and Fig. 6, it can be seen that the dielectric loss characteristics are the same, and there is no shift of the polarization peaks to the band of higher frequencies at M''. The fluid-paper insulation system does not change the dielectric response, which is presented by two parameters. It follows that the imaginary modulus for the fluid-paper system does not reveal polarization processes that were not recorded by the imaginary permittivity. Based on this, we find that the investigated frequency band is dominated by relaxation mechanisms and conduction losses suppressed by the losses of the relevant relaxation processes.

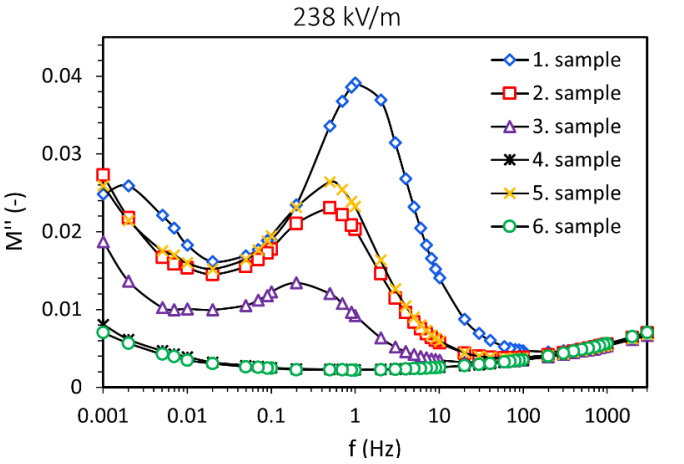

Figure 6

The frequency-dependent imaginary modulus $M''=f(f)$ of the investigated samples

3.3 Havriliak-Negami Plots

In subsections 3.1 and 3.2, the examined samples were subjected to complex permittivity and complex electric modulus analysis. The results indicate that polarization losses in the low-frequency band could suppress conduction losses. Modeling electrophysical processes will verify the given statement with the Havriliak-Negami function (hereinafter referred to as "H-N"). Based on this dielectric model, the conduction and polarization losses are described by the relations:

$$\varepsilon''_{DC}(\omega) = \frac{\sigma_{DC}}{i\omega\varepsilon_0} \tag{1}$$

$$\varepsilon''_{P}(\omega) = +Im\left\{\varepsilon_\infty + \frac{\varepsilon_S - \varepsilon_\infty}{[1+(i\omega\tau)^\alpha]^\beta}\right\} \tag{2}$$

considering that σ_{DC} represents the direct electrical conductivity, ω is the angular frequency, ε_0 is the vacuum permittivity, ε_s is the static or low-frequency permittivity ($\varepsilon'\to 0$), ε_∞ is the optical or high-frequency permittivity ($\varepsilon'\to\infty$), τ represents the time relaxations of the polarization process and α and β are empirical parameters describing the degree of distribution of relaxation times [17]. Fig. 7 shows the modeled curve of the 1. sample according to the H-N function. Modeling with approximation to the measured characteristic was performed with a deviation of 2.52%. The modeled characteristic is the sum of individual polarization losses ε''_{Px} and conduction losses ε''_{DC}. The modeled spectra prove that the polarization process is more dominant in the low-frequency band than in the conduction process.

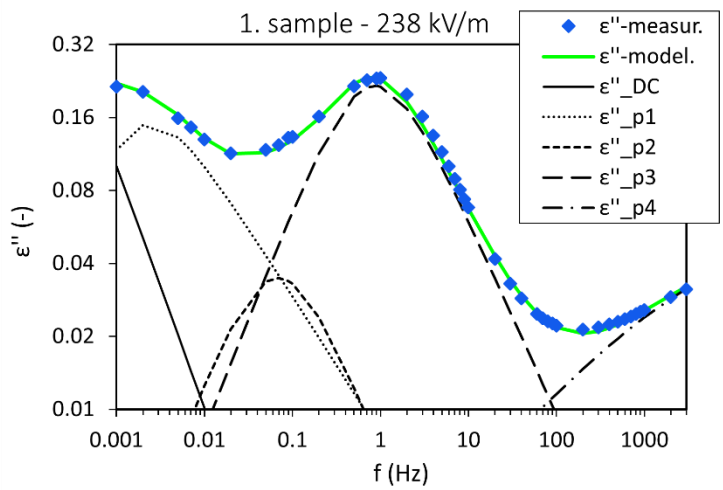

Figure 7
Modeling of electrophysical processes occurring in the 1. sample

The HIN-P insulation system responds to an applied electric field in the frequency band 1 mHz – 3 kHz by the presence of four polarization processes and a conduction process that is suppressed by relaxation losses. The polarization losses $\underline{\varepsilon''_{P1}}$ at a frequency of 2 mHz could be caused by the polarization of the space charge when applying a relatively high intensity alternating electric field. We estimate that the mentioned relaxation is not related to the fraction of Fe_3O_4 and C_{60} nanoparticles because the 6. sample without these nanoparticles shows a remarkable increase in dielectric losses in the low-frequency region (Fig. 12). The polarization process causes the contribution of dielectric losses $\underline{\varepsilon''_{P2}}$ at a frequency of 0.07 Hz. From Fig. 3 and Fig. 6, we see that the origin of the given relaxation is related to magnetic nanoparticles. Thus, it can be an interfacial polarization at the magnetic nanoparticle-oil interface. All investigated samples with a concentration of magnetic nanoparticles (HIN-P and 5. sample) show similar behavior with this polarization at a frequency of 0.07 Hz. Fullerene nanoparticles do not cause this process because the 5. sample without these nanoparticles supports the occurrence of $\underline{\varepsilon''_{P2}}$ polarization losses (Fig. 11). Another proof is the characteristic of the 4. sample without magnetic nanoparticles (with C_{60} 0.01 %w/V), which has no $\underline{\varepsilon''_{P2}}$ contribution (Fig. 10). The most significant influence of polarization losses on the dielectric response is present around the frequency of 1 Hz. The polarization losses $\underline{\varepsilon''_{P3}}$ are related to the electric double layer polarization that occurs in ferrofluids at frequencies close to 1 Hz [8] [12] [18-20]. Magnetic nanoparticles are stabilized by a surfactant whose head is polar, creating a negatively charged particle. This system forms the first electrical layer that electrostatically attracts the positive ions present in the nanofluid. This mechanism supports the formation of a second electric layer on the nanoparticle's surface, which polarizes the system under an applied electric

field. By increasing the frequency, further increase of polarization losses in the band 100 Hz – 3 kHz is investigated. The contribution $\underline{\varepsilon''_{P4}}$ causes interfacial fluid-paper polarization. This is confirmed by the finding from Fig. 3 and Fig. 6, which reveals a high-frequency increase in dielectric loss for every sample investigated, even for (6 sample) (NIN-P) without magnetic and fullerene nanoparticles. The individual relaxation parameters involved in modeling the H-N function are listed in Tab. 2.

Fig. 8 shows the modeling of electrophysical processes of the 2. HIN-P sample. We state that the deviation of the modeled characteristic from the measured characteristic is equal to 3.3%. The lower the deviation, the more accurate the values of the modeling parameters of the characteristic $\underline{\varepsilon''_{model.}}$ given in Tab. 2. The (2 sample) differs from the (1 sample) in the increased concentration of fullerene nanoparticles by 0.01 %w/V (C_{60} = 0.02 %w/V). With this sample, we capture the same types of electrophysical processes as in Fig. 7.

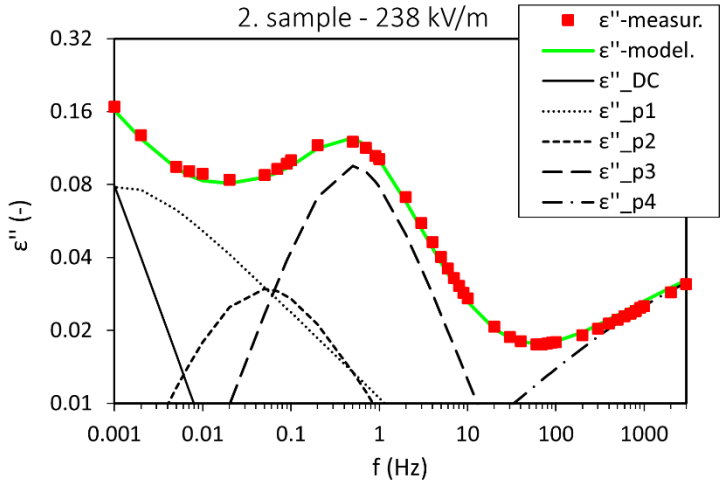

Figure 8
Modeling of electrophysical processes occurring in the 2. sample

Modeling of electrophysical processes of the 3. sample HIN-P is shown in Fig. 9. We note that the deviation of the modeled curve from the measured curve is equal to 2.63%. Similarly, as with samples 1 and 2, the same types of electrophysical processes are present. The difference is that the increase in the concentration of fullerene nanoparticles in HIN-P limits the contributions of $\underline{\varepsilon''_{P1}}$, $\underline{\varepsilon''_{P2}}$, and $\underline{\varepsilon''_{P3}}$, thereby reducing the dielectric losses and shifting these contributions to lower frequencies. Dielectric losses are also reduced at operating frequencies of 50 Hz and 60 Hz, which is a remarkable feature in the potential application of these samples.

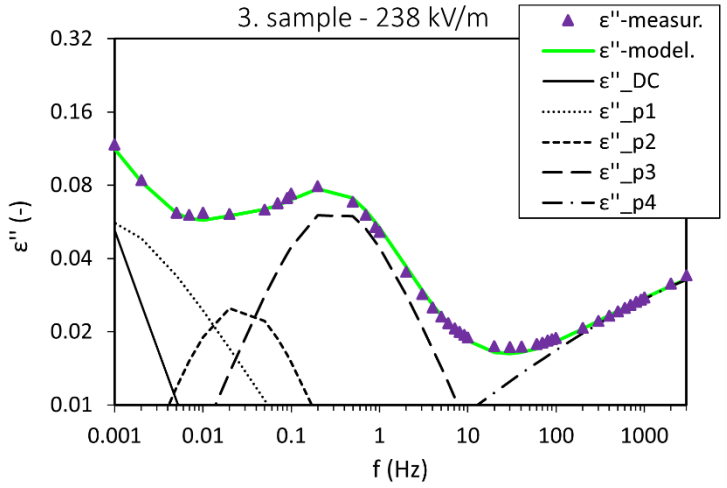

Figure 9

Modeling of electrophysical processes occurring in the 3. sample

In Fig. 10, we show the modeling of electrophysical processes of the (4 sample) NIN-P, which has only the fullerene fraction. We state that the deviation of the modeled characteristic from the measured characteristic is equal to 2.64%. This sample does not show the contributions of polarization losses ε''_{P2} and ε''_{P3} because it does not contain magnetic nanoparticles, like samples HIN-P and (5 sample). We register only space charge polarization and fluid-paper interfacial polarization. The parameter values are recorded in Tab. 2.

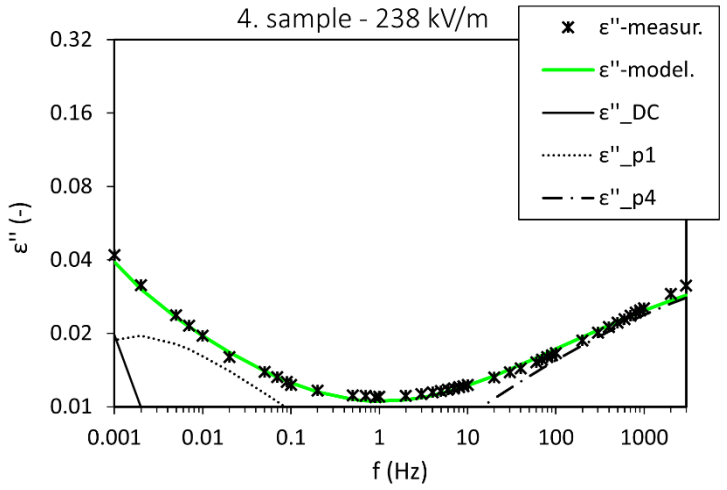

Figure 10

Modeling of electrophysical processes occurring in the 4. sample

Modeling of sample 5 NIN-P, which contains exclusively magnetic nanoparticles, is presented in Fig. 11. The occurrence of types of electrophysical processes is the same as for HIN-P samples. It is, therefore, evident that fullerene nanoparticles are not responsible for the contribution of polarization losses $\underline{\varepsilon''_{P2}}$ and $\underline{\varepsilon''_{P3}}$, which would cause a reduction of their contributions with a shift in the frequency spectrum. The deviation of the modeled characteristic of sample 5, is at the level of 3.82%.

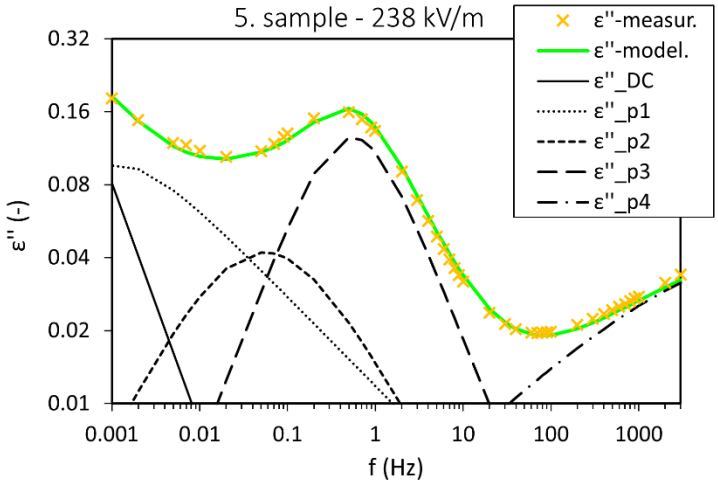

Figure 11
Modeling of electrophysical processes occurring in the 5. sample

Fig. 12 shows the modeled characteristics of the sample 6 NIN-P, which does not contain any concentration of nanoparticles. It consists exclusively of an oil-paper system. We note that the deviation of the modeled characteristic is equal to 3.69%. Similarly, as with sample 4, we do not register the contributions of polarization losses $\underline{\varepsilon''_{P2}}$ and $\underline{\varepsilon''_{P3}}$. Sample 4, which differs from sample 6, with the presence of fullerene nanoparticles, shows an increase in the contribution of polarization losses $\underline{\varepsilon''_{P1}}$ and conduction losses $\underline{\varepsilon''_{DC}}$. This is due to the fullerene fraction, which causes a higher conductivity of the material and a higher polarizability of the space charge in the low-frequency band of dielectric losses.

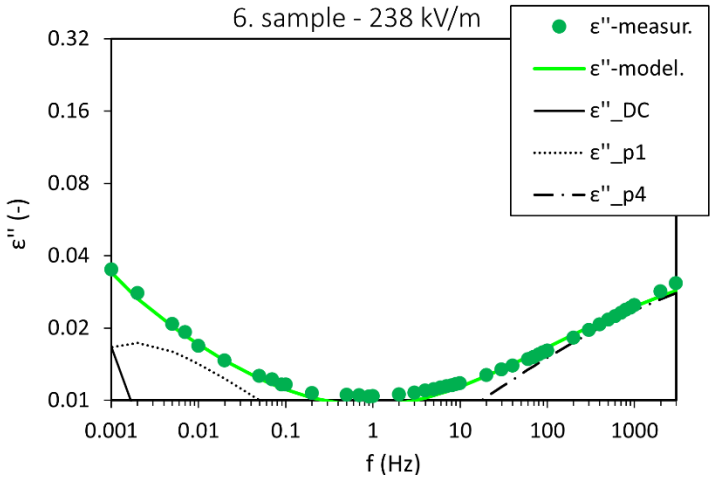

Figure 12
Modeling of electrophysical processes occurring in the 6. sample

As mentioned above in the text, Tab. 2 shows the parameter values of electrophysical process modeling of hybrid and non-hybrid nanofluid-paper insulation system samples using the H-N function. These parameters were modeled through equations (1) and (2). We note that the deviations mentioned above during modeling would slightly change the values of the individual parameters of the $\varepsilon''_{model.}$ characteristic.

Table 2
Parameter values of modeling electrophysical processes through the H-N function

sample	parameter	p1	p2	p3	p4
1.	ε_s (-)	3.06	2.65	2.69	2.16
	ε_∞ (-)	2.65	2.57	2.17	1.512
	α (-)	0.96	0.925	0.921	0.412
	β (-)	0.6	0.95	0.881	0.201
	τ (s)	100.2	2.449	0.205	0.000022
2.	ε_s (-)	2.65	2.67	2.35	2.3
	ε_∞ (-)	2.36	2.58	2.14	1.65
	α (-)	0.91	0.8	0.95	0.36
	β (-)	0.39	0.79	0.96	0.23
	τ (s)	301.4	4.123	0.338	0.000022
3.	ε_s (-)	2.55	2.64	2.525	2.39
	ε_∞ (-)	2.37	2.58	2.365	1.59
	α (-)	0.81	0.91	0.87	0.31
	β (-)	0.69	0.96	0.95	0.22
	τ (s)	312.5	6.373	0.538	0.000022

4.	ε_s (-)	2.305	-	-	2.21
	ε_∞ (-)	2.21	-	-	1.64
	α (-)	0.81	-	-	0.29
	β (-)	0.31	-	-	0.29
	τ (s)	305.8	-	-	0.000022
5.	ε_s (-)	2.72	2.72	2.61	2.3
	ε_∞ (-)	2.37	2.58	2.33	1.65
	α (-)	0.9	0.7	0.94	0.36
	β (-)	0.41	0.95	0.97	0.23
	τ (s)	301.6	3.154	0.304	0.000022
6.	ε_s (-)	2.303	-	-	2.21
	ε_∞ (-)	2.22	-	-	1.64
	α (-)	0.85	-	-	0.3
	β (-)	0.29	-	-	0.28
	τ (s)	306.2	-	-	0.000022

Conclusions

This study analyzed modern insulating materials based on the fluid-paper system. Hybrid and non-hybrid insulation systems were studied using the dielectric relaxation spectroscopy method in the frequency domain. These are unique results in the diagnostics of insulation materials for high-voltage applications, as samples of hybrid and non-hybrid nanofluids with different types and combinations of nanoparticles that formed a single unit with cellulose insulation were investigated and compared. Such materials are not sufficiently researched; therefore, the added value of this publication is precisely the research of the given modern insulation system. Frequency-dependent dielectric spectroscopy showed that dielectric losses in hybrid insulation systems could be reduced by increasing the concentration of fullerene nanoparticles. Increasing fullerene nanoparticles limited the contributions of relaxation processes such as interfacial polarization at the magnetic nanoparticle-fluid interface and electric double layer polarization. The presence of electrical double layer polarization was responsible for increasing dielectric losses at industrial frequencies of 50Hz and 60Hz. Therefore, the stated finding is sympathetic to the potential application of the studied samples in practice. In the opposite case, in the non-hybrid nanofluid-paper system, there was an increase in dielectric losses at the concentration of fullerene nanoparticles with a fraction of 0.01 %w/V, mainly in the low-frequency band.

This study also showed that the complex electric modulus in the fluid-paper system does not shift the relaxation information to higher frequencies compared to the complex permittivity. Their dielectric responses ranged at the same frequencies. Therefore, it is possible to analyze these systems with one complex parameter and use the modeling of electrophysical processes through the Havriliak-Negami function. Based on this function, the parameter values of individual electrophysical

processes, which make up the frequency spectrum of the studied modern materials, were revealed. The liquid-paper insulating system with a concentration of magnetic nanoparticles exhibits four polarization processes and one conduction process in the frequency spectrum of 1 mHz – 3 kHz. The examined frequency spectrum of samples without magnetic nanoparticles contains two polarization processes and one conduction process. Individual types of polarization processes were presented in the results of this study. This work also provides a springboard for continuing research into these modern insulation systems. It is necessary to experimentally verify the behavior of these materials under various degradation factors and through several diagnostic methods for a comprehensive description of changes in the electrophysical structure of the given modern material. Dielectric relaxation response in the frequency band at the operating temperatures of the power transformer, with the application of these temperatures in a specific time horizon, would be no less important information concerning the insulating state of these materials.

Acknowledgement

This research was funded by the Ministry of Education, Youth and Sports within the project VEGA 2/0011/20 and 1/0154/21 and the Slovak Agency for Research and Development based on contracts no. APVV-15-0438, APVV-17-0372, and APVV-18-0160.

References

[1] H. Hu et al.: Association rule mining from failure analysis test reports of transformers, The 16th IET International Conference on AC and DC Power Transmission (ACDC 2020), 2020, pp. 2101-2105

[2] O. Kulakov, A. Katunin, M. Kustov, E. Slepuzhnikov and S. Rudakov: Investigation of Reliability of Emergency Shutdown of Consumers in Electric Power Systems of Explosive Hazardous Zones, 2022 IEEE 3rd KhPI Week on Advanced Technology (KhPIWeek), 2022, pp. 1-5

[3] Z. Čonka, V. Kohan, M. Kolcun, P. Judith and I. J. Rudas: Fault localization method using WAM systems, 2020 21st International Scientific Conference on Electric Power Engineering (EPE), 2020, pp. 1-4

[4] IEEE Standard for Liquid-Immersed Transformers Designed to Operate at Temperatures Above Conventional Limits Using High- Temperature Insulation Systems - Redline, in IEEE Std C57.154-2022 (Revision of IEEE Std C57.154-2012) – Redline, 18 Aug. 2022, pp. 1-96

[5] M. Rajňák, J. Kurimský, R. Cimbala, Z. Čonka, P. Bartko, M. Šuga, K. Paulovičová, J. Tóthová, M. Karpets, P. Kopčanský, M. Timko: Statistical analysis of AC dielectric breakdown in transformer oil-based magnetic nanofluids, Journal of Molecular Liquids, Vol. 309, July 2020, pp. 113243-1-7

[6] M. Rafiq, M. Shafique, A. Azam, M. Ateeq: Transformer oil-based nanofluid: The application of nanomaterials on thermal, electrical and physicochemical properties of liquid insulation-A review, Ain Shams Engineering Journal, Vol. 12, 2021, pp. 555-576

[7] S. S. Leong, Z. Ahmad and JK Lim: Magnetophoresis of superparamagnetic nanoparticles at low field gradient: hydrodynamic effect, Soft Matter, Vol. 11, 2015, pp. 6968-9680

[8] R. Cimbala, P. Havran, J. Király, M. Rajňák, J. Kurimský, M. Šárpataky, B. Dolník, K. Paulovičová: Dielectric response of a hybrid nanofluid containing fullerene C_{60} and iron oxide nanoparticles, Journal of Molecular Liquids, Vol. 359, May 2022, pp. 1-9

[9] K. Paulovičová, J. Tóthová, M. Rajňák, M. Timko, P. Kopčanský, V. Lisý: Nanofluid Based on New Generation Transformer Oil: Synthesis and Flow Properties, ACTA PHYSICA POLONICA A, Vol. 137, May 2020, pp. 908-910

[10] P. Havran, R. Cimbala, J. Kurimský, B. Dolník, I. Kolcunová, D. Medveď, J. Király, V. Kohan, Ľ. Šárpataky: Dielectric Properties of Electrical Insulating Liquids for High Voltage Electric Devices in a Time-Varying Electric Field, Energies, Vol. 15, 391, Jan. 2022, pp. 1-21

[11] Shell Lubricants, Technical Paper, Available online: file:///C:/Users/phavr/Downloads/diala-white-paper-low.pdf (accessed on 24 September 2022)

[12] M. Rajňák, J. Kurimský, B. Dolník, P. Kopčanský, N. Tomašovičová, E. A. Taculescu-Moaca, M. Timko: Dielectric-spectroscopy approach to ferrofluid nanoparticle clustering induced by an external electric field, Physical Review E, Vol. 90, Sept. 2014, pp. 032310-1-9

[13] M. Wübbenhorst, J. Turnhout: Analysis of complex spectra. I. One-dimensional derivative techniques and three-dimensional modeling, Journal of Non-Crystalline Solids, Vol. 305, July 2002, pp. 40-49

[14] L. Sheng-Tao, W. Hui, L. Chun-Jiang, L. Jian-Ying: Dielectric modulus response of CaCu3Ti4O12 ceramic, Acta Physica Sinica, Vol. 62, Aug. 2013, pp. 087701-1-6

[15] I. M. Ward: Anelastic and dielectric effects in polameric solids, Wiley: New York and London, 1967

[16] K. Yang, M. Dong, Y. Hu, J. Xie, M. Ren: The Application of Dielectrc Modulus in the Oil-impregnated Paper Insulation, 2020 Elect. Insul. Conf. (EIC), IEEE press, Knoxville TN USA, 05 Aug. 2020, pp. 103-106

[17] J. Xie, M. Dong, Y. Hu, T. Zhuang, R. Albarracín-Sánchez, J.M. Rodríguez-Serna: Modeling Oil-paper Insulation Frequency Domain Spectroscopy

Based on its Microscopic Dielectric Processes, IEEE Transactions on Dielectrics and Electrical Insulation, Vol. 26, Dec. 2019, pp. 1788-1796

[18] R. P. Misra, S. Das, S. K. Mitra: Electric double layer force between charged surfaces: Effect of solvent polarization, The Journal of Chemical Physics, Vol. 138, Mar. 2013, pp. 114703

[19] Š. Hardoň, J. Kúdelčík, M. Gutten: Dielectric Spectroscopy of Two Concentrations of Magnetic Nanoparticles in Oil-Based Ferrofluid, Acta Physica Polonica A, Vol. 137, May 2020, pp. 961-963

[20] V. N. Shilov, A. V. Delgado, F. González-Caballero, J. Horno, J. J. López-García, C. Grosse: Polarization of the Electrical Double Layer. Time Evolution after Application of an Electric Field, Journal of Colloid and Interface Science, Vol. 232, Dec. 2000, pp. 141-148